

https://doi.org/10.1070/QEL16316

High-power optical parametric oscillator based on a high-pulse repetition rate, master Nd:KGW laser

M.V. Bogdanovich, A.V. Grigor'ev, K.I. Lantsov, K.V. Lepchenkov, A.G. Ryabtsev, G.I. Ryabtsev, M.A. Shchemelev, V.S. Titovets, L. Agrawal, A. Bhardwaj

Abstract. **An optical scheme of an optical parametric oscillator with a master laser based on an Nd:KGW active element excited by two orthogonally oriented diode side pump modules is proposed to form radiation pulses with energies above 30 mJ and a repetition rate of 1–20 Hz in the eye-safe spectral range of 1.5–1.6 μm. The two-module excitation of the active medium makes the distribution of the master laser radiation intensity in the output beam cross section more uniform and provides a reliable operation of the optical parametric oscillator.**

Keywords: *optical parametric oscillator, two-module diode side pumping, biaxial Nd:KGW crystal, eye-safe spectral range of 1.5–1.6 μm, radiation energy, pulse repetition rate.*

1. Introduction

Lasers with an active element (AE) based on ytterbium–erbium phosphate glass, excited in the side pump scheme by laser diode bars, proved to be efficient compact radiation sources for the eye-safe spectral range of 1.5–1.6 μm [1–4]. Nevertheless, their wide application in modern optoelectronic systems is limited in many respects by the low thermal conductivity of phosphate glass. For this reason, the output energy of ytterbium–erbium lasers is limited by a value of 8–10 mJ, especially when the pulse repetition rate f exceeds 5–10 Hz. Higher power, completely solid-state laser oscillators, reliably operating in the eye-safe spectral range at $f >$ 5–10 Hz, are generally designed using parametric conversion of the master Nd:YAG laser frequency. The use of a crystalline active medium makes it possible to design optical parametric oscillators (OPOs) with an output beam energy exceeding 50–60 mJ at a pulse repetition rate of 10–30 Hz [5–10]. However, the Nd:YAG crystal is characterised by a relatively narrow absorption band in the vicinity of λ = 810 nm, the wavelength to which the maximum of the spectral emission band of laser diode bars or arrays (LDBs or LDAs), used as pump sources, is tuned. This circumstance makes the requirements to the parameters of the LDB/LDA and the thermal stabilisation system of the diode pump unit more stringent and, in the long run, increases the cost of OPOs and reduces their competitiveness.

One of the ways to solve this problem is to use AEs based on the Nd:KGW crystal [11–16], whose absorption band in the vicinity of λ = 810 nm is wider than that of Nd:YAG by a factor of more than 5 [11–13]. The content of neodymium ions Nd^{3+} in Nd:KGW crystals can be increased to 4 at%–8 at% without any significant luminescence concentration quenching and change in the optical properties of the material. The absorption coefficient of pump radiation in Nd:KGW may exceed that for Nd:YAG by a factor of 1.5–2 [12, 13]. All these features open new possibilities for designing compact high-efficiency Nd:KGW lasers [13, 16–18]. Unfortunately, the aforementioned positive properties of the biaxial Nd:KGW crystal are partly invalidated by the effects initiated by the strong nonspherical thermal lens induced in the bulk of the active medium at high excitation levels and/or pump pulse repetition rates [19, 20]. It is noteworthy that, in the case of side AE excitation, the thermal lens configuration becomes even more complicated because of the nonuniform distribution of the pump radiation intensity in the AE bulk [21].

This study is devoted to the development and analysis of the characteristics of a pulsed OPO with a completely solid-state master laser based on an Nd:KGW crystal. The application of two orthogonally oriented diode pump modules (DPMs) in the Nd:KGW laser allows one to form an output beam with a symmetric (with respect to the cavity axis) intensity distribution and minimise the effects related to the inhomogeneous thermal lens induced in the AE. The OPO with a two-module pump scheme generates light pulses at λ = 1.57 μm with energy above 30 mJ and repetition rates in the range of 1–20 Hz.

2. Experiment and simulation of OPO operation

Figure 1 shows the optical scheme of the developed pulsed OPO operating in the eye-safe region. The scheme includes two identical DPMs, an electro-optic Q-switch, a 90° quartz rotator, an OPO cell and mirrors. Each DPM consists of a rectangular AE based on a Nd:KGW crystal side-pumped by two DPMs.

The experiments were performed using LDAs of SLM-3 type with a pulsed output power of 1.25 kW. All arrays were connected successively and excited by current pulses with durations τ_p = 100–200 μs and repetition rates f = 1–30 Hz. To stabilise the radiation wavelength in the vicinity of λ = 810 nm, LDAs were mounted on heat sinks, connected to the electronic temperature stabilisation system. The LDA emitting surface area was 5.0×25.0 mm in size.

M.V. Bogdanovich, A.V. Grigor'ev, K.I. Lantsov, K.V. Lepchenkov, A.G. Ryabtsev, G.I. Ryabtsev, M.A. Shchemelev, V.S. Titovets
B.I. Stepanov Institute of Physics, National Academy of Sciences of Belarus, prosp. Nezavisimosti 68, 220072 Minsk, Belarus;
e-mail: ryabtsev@dragon.bas-net.by;
L. Agrawal, A. Bhardwaj Laser Science and Technology Center, Delhi-110-054, India

Received 9 February 2017
Kvantovaya Elektronika **47** (4) 308–312 (2017)
Translated by Yu.P. Sin'kov

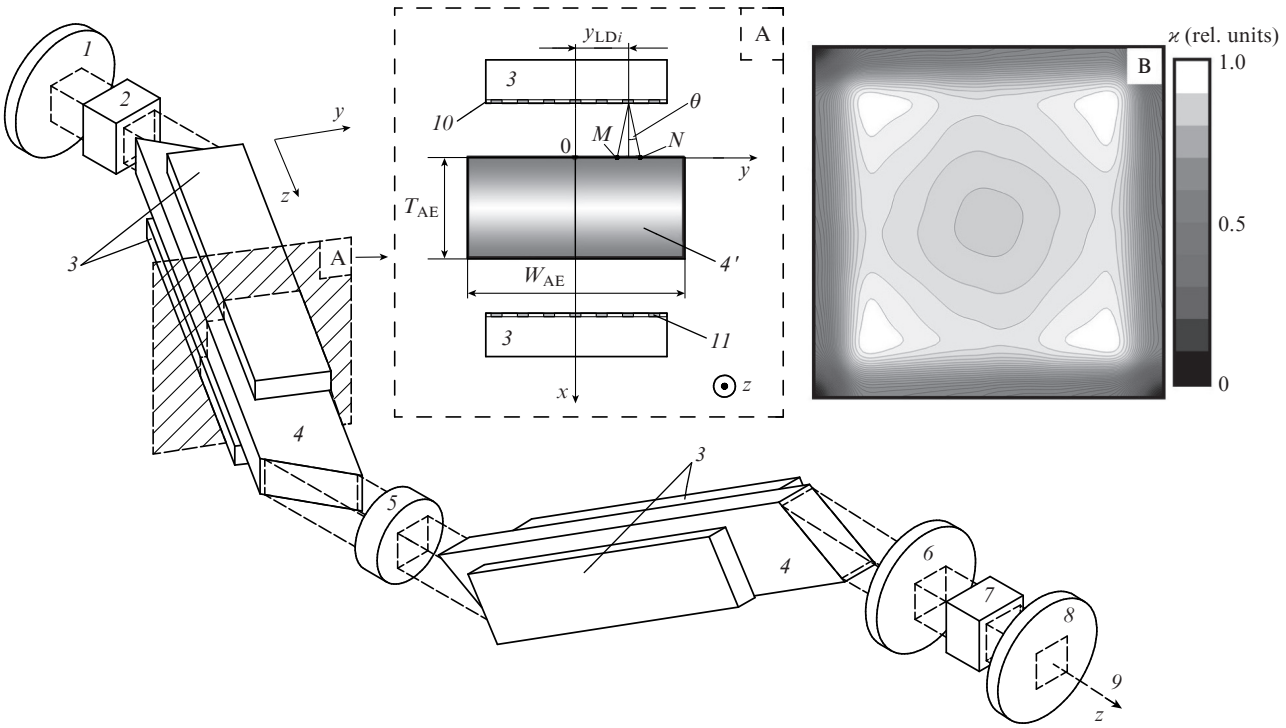

Figure 1. Optical scheme of the OPO based on an Nd:KGW laser: (*1*) highly reflecting spherical mirror of the master laser; (*2*) electro-optic *Q*-switch; (*3*) LDA; (*4*) AE [(*4′*) is the calculated distribution $I_a(x, y)$ formed by two LDAs in the AE cross section]; (*5*) 90° quartz rotator; (*6*) flat intermediate mirror; (*7*) MCT nonlinear crystal; (*8*) OPO output mirror; (*9*) OPO output beam; (*10*) heterostructure of individual LDB in LDA; (*11*) stripe LDB contacts; inset A shows the mutual arrangement of the LDAs and AE in the DPM cross section and inset B presents the spatial distribution of the master laser gain $\varkappa$ in the xy plane.

Nd:KGW crystals with a neodymium ion concentration of 3 at% were cut so as to make the principal axis N_p of the optical indicatrix coincide with the laser beam propagation direction in the crystal (i.e., with the cavity axis z) and the principal axis N_m coincide with the laser electric field vector [19]. The end faces of the crystalline AEs were bevelled at the Brewster angle; in this configuration, the maximum transmission was provided for the laser beam component with the electric vector oriented along the N_m axis. Both AEs had a length of 36.7 mm and a cross section $W_{AE} \times T_{AE}$ = 6.0×2.8 mm in size. The pump radiation was introduced into the AE bulk through the lateral faces 6.0×36.7 mm in size, which were made antireflective at a wavelength of 810 nm. This AE geometry provided an efficient heat removal through the lateral faces, which were not involved in the pump radiation supply.

The electro-optic *Q*-switch was chosen to be a Pockels cell with a nonlinear KD*P crystal. The radiation generated by the two-DPM master laser at λ = 1.067 μm was converted into radiation with a wavelength of λ = 1.570 μm according to the intracavity OPO conversion scheme. The OPO cell contained an MCT crystal 6×6×20 mm in size as a nonlinear element, with antireflection dielectric coatings at wavelengths of 1.067 and 1.570 μm, deposited on its lateral faces. All experiments were performed at room temperature.

DPMs rotated by 90° relative to each other were located pairwise along the master laser cavity axis z. This module configuration was mainly used to obtain a symmetric (with respect to the z axis) and maximally uniform distribution of the total radiation intensity $I_a(x, y)$ absorbed in the AE. The specific features of the spatial intensity distribution $I_e(z, y)$ in the LDA near field were taken into account within this approach. It was found that the highly divergent beams of the LDBs entering the composition of 2D LDAs [22] are almost completely overlapped along the z axis at a distance from the LDA emitting surface larger than 0.5–1.0 mm (Fig. 2); thus, a uniform intensity distribution $I_e(z, y)$ is provided along the cavity axis. Along the y axis, the $I_e(z, y)$ distribution exhibits a characteristic peak (denoted by letter *P* in Fig. 2), the origin of which is related to the specific features of current spreading in the SLM-3 design. To compensate for the influence of this peak on the pump intensity distribution in the active element,

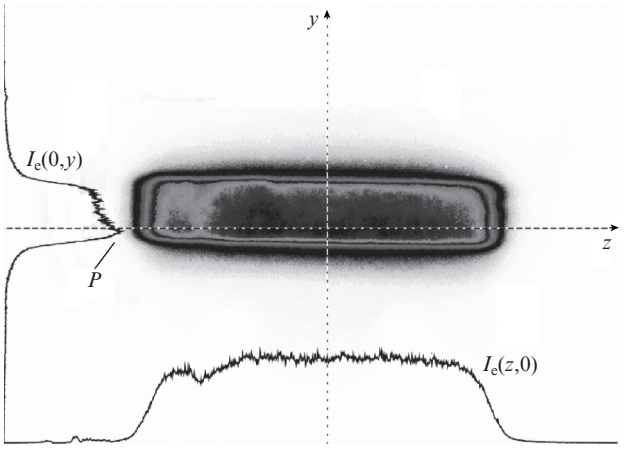

Figure 2. Radiation intensity distribution $I_e(z, y)$ for an LDA of SLM-3 type at a distance of 2.5 mm from the LDA emitting surface and cross sections of this distribution along the z and y axes.

the LDAs were chosen pairwise, with maximally similar shapes of the P peaks. The thus chosen LDAs were installed in the pump modules opposite the AE lateral faces, so that the P peaks fell on the opposite AE end faces. This approach made it possible to distribute more uniformly the pump energy in the AE volume along the y axis. The calculation results (Fig. 1, inset A) showed that the nonuniformity of the $I_a(x,y)$ distribution in the case under consideration is due to only the pump radiation absorption along the x axis.

To estimate the efficiency of the chosen master laser excitation scheme, we simulated the pump radiation propagation through the AE volume. Based on the experimental data presented in Fig. 2, we suggested that the LDA radiation intensity is uniformly distributed over the AE lateral surface along the z axis. On the assumption that the distribution of the output radiation intensity from individual emitters with a stripe contact geometry (which enter the LDBs forming the LDA) along the y axis is described by a Gaussian function and that the absorption along the x axis obeys the exponential law, the distribution of the absorbed radiation intensity in the AE cross section was presented in the form

$$I_a(x,y) = \sum_{i=1}^{N_{LD}} \frac{P_{0i}\exp(-\alpha x)}{\sqrt{\pi/2}\, w_i(x)} \exp\left[-\frac{2(y-y_{LDi})^2}{w_i^2(x)}\right], \quad (1)$$

where N_{LD} is the number of individual emitters (laser diodes); P_{0i} is the power of an individual ith emitter; is the effective absorption coefficient of Nd:KGW at $\lambda = 810$ nm; $w_i(x) = w_{0i} + (x/n)\tan\theta$ is the beam FWHM for the ith emitter as a function of coordinate x; w_{0i} is the beam width for the ith emitter on the AE lateral surface in the direction of the y axis (Fig. 1, inset A, segment MN); n is the Nd:KGW refractive index; and y_{LDi} is the coordinate along the y axis of the ith-emitter stripe contact centre. The P_{0i} and y_{LDi} values were determined experimentally. Note that expression (1) sets the $I_a(x,y)$ distribution formed by LDA from only one side of the AE. It was assumed that the $I_a(x,y)$ distribution formed by the LDA on the opposite lateral side of the AE has a similar form. The result of simulating the joint action of two LDAs is illustrated by the total intensity distribution $I_a(x,y)$ of the pump radiation absorbed in the AE (Fig. 1, inset A, position 4′).

The geometric parameters W_{AE} and T_{AE} of both active elements were chosen so as to make the beam emerging from the end face of the Nd:KGW crystal (beveled at the Brewster angle) have a square cross section. Proceeding from the width of the LDA emitting area (5.0 mm along the y axis, see Fig. 2), the W_{AE} value was taken to be 6.0 mm; the size of the AE excitation region along the y axis was 5.0 mm. With allowance for the chosen width W_{AE} and the Nd:KGW refractive index at $\lambda = 1.067$ μm ($n_{AE} = 1.986$ [23]) and on the assumption that no less than 80% pump radiation is absorbed in one pass, the active element thickness T_{AE} was taken to be 2.8 mm.

According to the master laser optical scheme, the electric field vector for the beam with a square cross section, emerging from the end face of the AE in the first DPM (it is shown in the left part of the scheme in Fig. 1), is rotated by 90° after the beam transmission through quartz rotator (*5*). Then the laser beam (with minimum optical loss) arrives at the AE of the second DPM and is transformed into a beam with a rectangular cross section. However, the AE in the second DPM is excited through lateral sides (along the y axis), which are rotated by 90° with respect to the sides of the AE in the first DPM. As a result, the spatial distribution of the master laser gain in the xy plane becomes symmetric with respect to z axis (Fig. 1, inset B).

To test experimentally the operational efficiency of the master laser with two DPMs (type II), its characteristics were compared with those of the Nd:KGW laser equipped with a single DPM (type I), at comparable levels of active medium excitation.

Using the standard system of rate equations for the inverse population and the number of emitted photons [24], we determined the parameters of the Nd:KGW master laser cavity at which the lasing energy E_{las} reaches a maximum. In this way, we found the optimal values of mirror reflectivities for the two versions of master laser: with one DPM and with two DPMs. The data obtained were used to match the waist of the master laser mode with the sizes of the nonlinear MCT crystal in the OPO cell and its position along the z axis. As a result, highly reflecting (at $\lambda = 1.067$ μm) mirror (*1*) (Fig. 1) was chosen to be a spherical mirror with a radius of curvature of 500 mm. Output plane mirror (*6*) was made antireflective at a wavelength of 1.067 μm, with a maximum reflectance at 1.57 μm. The reflectance of output mirror (*8*) of the OPO cell was ~99.5% at $\lambda = 1.067$ μm and ~70% at $\lambda = 1.57$ μm. The length of the Nd:KGW master laser cavity was 150 or 250 mm in the schemes with one or two DPMs, respectively.

To compare the energy characteristics of the master lasers of types I and II under comparable pump conditions, the DPM of the I-type laser was excited by current pulses with a duration $\tau_p = 200$ μs, whereas the DPM of the II-type laser was excited by pulses with $\tau_p = 100$ μs. Since LDAs were connected successively in all cases, identical values of the pump energy E_{pm} were obtained by applying current pulses with identical amplitudes to the DPMs (the variations in the light–current characteristics of the LDAs in use did not exceed few percent).

The dependence of the output energy of the OPOs with master lasers of types I and II (E_I and E_{II} values, respectively) on the pump level and pulse repetition rate was studied experimentally. The OPO pulse duration was 7 ns.

3. Results and discussion

As can be seen in Table 1, at identical pump energies, master lasers of types I and II generate pulses with comparable energies if $f \leqslant 10$ Hz. However, with a further increase in the pulse repetition rate, the E_I and E_{II} values significantly differ. For example, with an increase in f from 10 to 20 Hz, the output pulse energy for the two-DPM OPO ($E_{pm} = 520$ mJ) decreases by less than 4% (from 35.4 to 34.0 mJ), whereas the pulse energy for the one-DPM OPO decreases from 31.0 mJ to zero.

Table 1. Energies E_I and E_{II} of the output pulses of the OPO based on a master Nd:KGW laser with one and two DPMs, respectively, depending on the pulse repetition rate f (both lasers operated in the Q-switching regime at $E_{pm} = 520$ mJ).

E_I/mJ	E_{II}/mJ	f/Hz
31.1	37.1	1
31.1	36.3	5
31.0	35.4	10
2.5	35.4	15
0	34.0	20

A joint analysis of the E_I and E_{II} values (measured at different rates f) and the near-field patterns of Nd : KGW master lasers of types I and II suggests that a sharp decrease in E_I at $f > 10$ Hz is mainly due to the formation of a strongly anisotropic thermal lens in the AE volume and, as a consequence, the violation of the cavity stability. The intensity distribution in the output beam cross section for the type-I master laser becomes nonuniform even at relatively low AE excitation levels. With an increase in the LDA pump current and/or pulse repetition rate, the nonuniformity of this distribution rapidly increases. In contrast to this case, the intensity of the radiation of the II-type master laser (for all operation regimes and E_{pm} and f values under study) is distributed relatively uniformly over the beam cross section and exhibits a pronounced symmetry with respect to the z axis (Fig. 3). The experimental near-field patterns for the II-type laser correlate with the model gain distribution in the xy plane at the output of the second DPM, which is presented in inset B in Fig. 1. Note also that the II-type laser is characterised by a higher ($\sim$1%) amplitude stability of generated pulses in comparison with the I-type laser.

The elimination of the pronounced 'hot' points in the near-field pattern of the II-type Nd : KGW master laser reduces the probability of optical breakdown in the bulk of the nonlinear MCT crystal, due to which the oscillator reliability essentially increases.

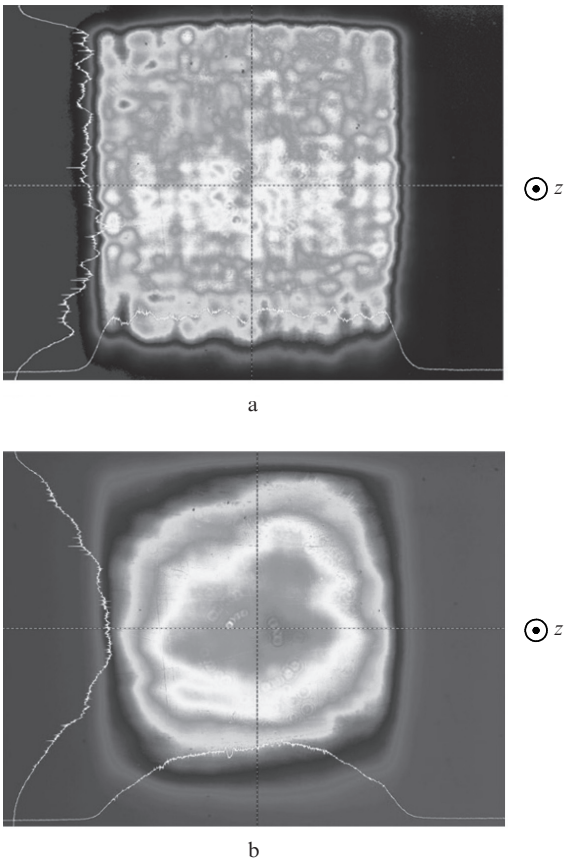

Figure 3. Near-field patterns of intensity distribution for the II-type Nd : KGW master laser (λ = 1.067 μm) in the (a) free-lasing regime and (b) Q-switching regime at f = 20 Hz. The laser pulse energies are (a) 110 and (b) 70 mJ. The patterns were recorded by a CCD camera located at a distance of 40 mm from intermediate mirror (*6*) [before starting the measurements, nonlinear crystal (*7*) and output mirror (*8*) were removed from the scheme (Fig. 1)].

4. Conclusions

An optical scheme of an OPO based on a Nd : KGW master laser with two orthogonally oriented diode side pump modules was proposed to generate pulses with energies above 30 mJ and repetition rates up to 20 Hz in the eye-safe spectral range of 1.5–1.6 μm. The two-module excitation of the active medium makes the intensity distribution in the master laser beam cross section more uniform and provides an OPO pulse energy at a level of 30–35 mJ in the range of pulse repetition rates of 1–20 Hz. In this case, the increase in the uniformity of the intensity distribution in the near-field zone is due to the fact that the excitation in each DPM occurs through different pairs of the rectangular AE lateral faces. The symmetry of the Nd : KGW laser near-field pattern with respect to the cavity axis facilitates the formation of a thermal lens in the active medium; this lens is characterised by stable optical parameters in a wide range of excitation energies and pump pulse repetition rates. As a result, the high energies of the output OPO pulses are maintained approximately constant without any additional alignment of the master laser cavity.

References

1. Ryabtsev G.I., Bezyazychnaya T.V., Bogdanovich M.V., Grigor'ev A.V., Kabanov V.V., Lebiadok Y.V., Ryabtsev A.G., Shchemelev M.A. *Appl. Phys. B*, **108**, 283 (2012).
2. Ryabtsev G.I., Bogdanovich M.V., Grigor'ev A.V., Kabanov V.V., Lebedok E.V., Lepchenkov K.V., Ryabtsev A.G., Shchemelev M.A. *Opt. Zh.*, **82**, 3 (2015).
3. Cole B., Hough N., Hays A., Nettleton J., Goldberg L. *Proc. SPIE*, **9726**, 972605 (2015).
4. Bogdanovich M.V., Grigor'ev A.V., Lantsov K.I., Lepchenkov K.V., Ryabtsev A.G., Ryabtsev G.I., Titovets V.S., Shchemelev M.V. *Fotonika*, **55**, 58 (2016).
5. Wang Y.Y., Xu D.G., Zhong K., Wang P., Yao J.Q. *Appl. Phys. B*, **97**, 439 (2009).
6. Bhardwaj A., Agrawal L., Maini A.K. *Defence Sci. J.*, **63**, 599 (2013).
7. Iskandarov M.O., Nikitichev A.A., Sverdlov M.A., Ter-Martirosyan A.L. *Nauchn. Priborostr.*, **25**, 124 (2015).
8. Zhong K., Wang Y.Y., Xu D.G., Geng Y.F., Wang J.L., Wang P., Yao J.Q. *Chin. Phys. Lett.*, **26**, 064210 (2009).
9. Wu F.F., Pierce J.W. *Proc. SPIE*, **7582**, 75820H (2010).
10. Cho C.Y., Chen Y.C., Huang Y.P., Huang Y.J., Su K.W., Chen Y.F. *Opt. Express*, **22**, 7625 (2014).
11. Kaminsky A.A. *Lazernye kristally* (Laser Crystals) (Moscow: Nauka, 1975).
12. Batai L.E., Gribkovskii V.P., Demidovich A.A., Kuz'min A.N., Ryabtsev G.I. *Izv. NANB, Ser. Fiz.-Mat. Nauk*, **4**, 82 (1998).
13. Kushawaha V., Michael A., Major L. *Appl. Phys. B*, **58**, 533 (1994).
14. Chen Y., Major L., Kushawaha V. *Appl. Opt.*, **35**, 3203 (1996).
15. Demidovich A.A., Shkadarevich A.P., Batay L.E., Gribkovskii V.P., Kuzmin A.N., Ryabtsev G.I., Stek W., Deren P. *Proc. SPIE*, **3176**, 272 (1997).
16. Demidovich A.A., Shkadarevich A.P., Danailov M.B., Apai P., Gribkovskii V.P., Kuzmin A.N., Ryabtsev G.I., Batay L.E. *Appl. Phys. B*, **67**, 11 (1998).
17. Demidovich A.A., Kuzmin A.N., Ryabtsev G.I., Stek W., Titov A.N. *Spectrochim. Acta, Part A*, **54**, 1711 (1998).
18. Grabtchikov A.S., Kuzmin A.N., Lisinetskii V.A., Ryabtsev G.I., Orlovich V.A., Demidovich A.A. *J. Alloys Comp.*, **300-301**, 300 (2000).

19. Yumashev K.V., Savitski V.G., Kuleshov N.V., Pavlyuk A.A., Molotkov D.D., Protasenya A.L. *Appl. Phys. B*, **89**, 39 (2007).
20. Berger J.A., Greco M.J., Schroeder W.A. *Opt. Express*, **16**, 8629 (2008).
21. Bezyazychnaya T.V., Bogdanovich M.V., Grigor'ev A.V., Kabanov V.V., Kostik O.E., Lebiadok Y.V., Lepchenkov K.V., Mashko V.V., Ryabtsev A.G., Ryabtsev G.I., Shchemelev M.A., Teplyashin L.L. *Opt. Commun.*, **308**, 26 (2013).
22. Botes D., Scrifres D.R. (Eds) *Diode Laser Arrays* (Cambridge: Cambridge University Press, 1994).
23. http://eksmaoptics.com/.
24. Koechner W. *Solid-State Laser Enginering* (New York: Springer, 2002) Ch. 8.